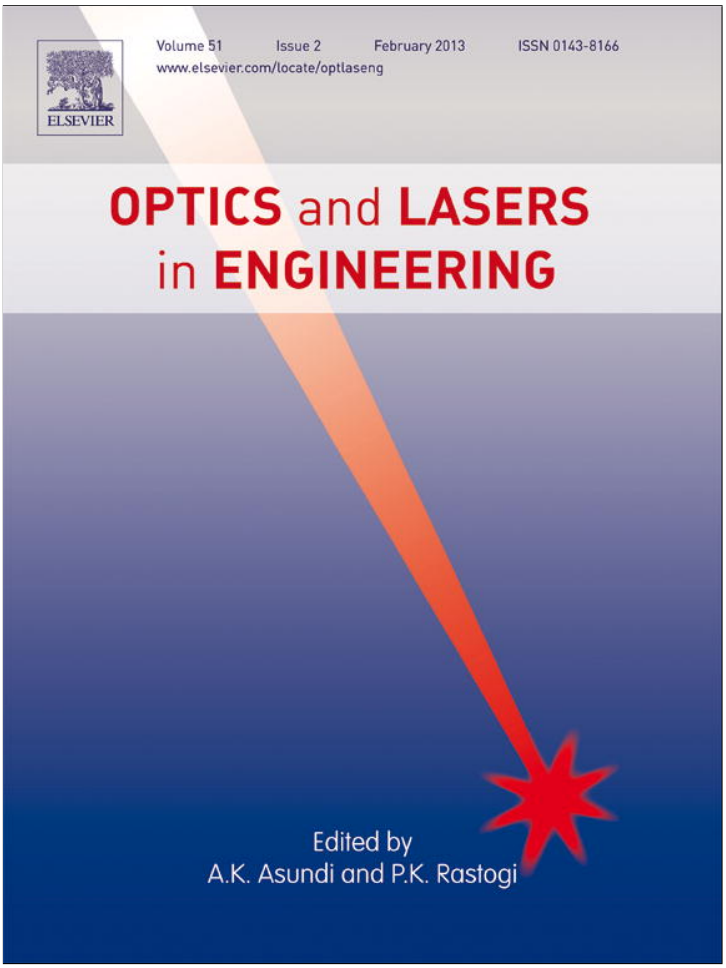

Optics and Lasers in Engineering 51 (2013) 111–115

Contents lists available at SciVerse ScienceDirect

Optics and Lasers in Engineering

journal homepage: www.elsevier.com/locate/optlaseng

Second order diffractive optical elements in a spatial light modulator with large phase dynamic range

Jorge Albero [a,*], Pascuala García-Martínez [b], José Luis Martínez [a], Ignacio Moreno [a]

[a] Universidad Miguel Hernández, Departamento de Ciencia de Materiales, Óptica y Tecnología Electrónica, Av. Universidad S/N, Ed. Torrevaillo, 03202 Elche, Alicante, Spain
[b] Departamento de Óptica, Universitat de València, 45100 Burjassot, Spain

ARTICLE INFO

Article history:
Received 13 July 2012
Received in revised form
6 September 2012
Accepted 7 September 2012
Available online 28 September 2012

Keywords:
Spatial light modulators
Diffraction gratings
Diffractive lenses
Phase shift

ABSTRACT

A study of the diffraction efficiency of a spatial light modulator with a large dynamic phase range is reported. We use a phase-only device that reaches 4π phase modulation depth for the wavelength of 454 nm. This allows operating phase-only diffractive optical elements in the second harmonic diffraction order, instead of in the usual first diffraction order. This type of implementation shows advantages in terms of resolution and diffraction efficiency. Experimental results are reported for blazed diffractive gratings and diffractive lenses.

1. Introduction

Diffractive optical elements (DOEs) play an important role in many optical technologies [1]. Liquid crystal (LC) spatial light modulators (SLMs) are useful devices for implementing a variety of programmable DOE, mainly when they produce pure-phase modulation characteristics [2]. Usually, a pure phase-only modulation with a phase modulation range reaching 2π radians is desired. Initial works in this field involved twisted nematic and parallel-aligned LC-SLMs [3,4]. The goal of reaching faster optical responses led to a reduction of the liquid crystal layer in modern devices. This motivated the use of elliptical polarization configurations to achieve a phase-only regime [5], but it reduced the overall phase modulation range. In some devices, the available phase dynamic range is actually shorter than 2π radians in standard configurations. Strategies have been demonstrated either to optimally encode a phase-DOE onto a limited phase modulation device [6], or to enlarge the phase modulation range by unconventional polarization configuration, this phase improvement requiring a reduction of the average intensity transmission [7].

Modern LC on Silicon (LCoS) modulators work in reflection, thus providing larger values of the phase modulation range. In addition, some LCoS devices like parallel-aligned nematic (PAL), or vertically aligned nematic (VAN) act as electrically controlled birefringence (ECB) displays, i.e., programmable linear wave-plates. Phase-only modulation is therefore obtained in these devices simply by orienting the input linear polarization parallel to the LC director axis. Therefore, phase-only LC devices with phase modulation range larger than 2π are nowadays commercially available.

In this paper, we examine the diffraction properties of two-dimensional DOEs displayed in a parallel-aligned LCoS display with a dynamic phase range reaching 4π radians. This doubled phase depth, compared to standard 2π phase modulation, allows operating DOEs in the second harmonic diffraction order. It is shown that this operation presents advantages in terms of spatial resolution. For example, it permits reducing the diffraction efficiency loss induced when the displayed DOE presents high spatial frequency components, near the resolution limit of the device [8,9].

The paper is organized as follows. First, in the next section we examine the theory for the blazed grating with different phase modulation depth, in particular when the phase range exceeds the usual 2π range. Then, in Section 3 we present experimental results obtained with a phase-only LCoS display, capable of reaching 4π phase modulation for an operating wavelength of 454 nm. We show how the blazed grating can be operated in the second harmonic component. Then, the approach is extended to other diffractive elements, in particular to a diffractive lens. We show that operating in this second harmonic component improves the diffraction efficiency of the displayed lens. Finally, the last section presents the conclusion of the work.

2. Blazed grating with variable phase depth

Let us first analyze a one dimensional blazed phase diffraction grating. It can be expressed as a linear phase dependence

$$g(x) = \exp\left(i\varphi(x)\right) = g_0(x) \otimes \frac{1}{p}\mathrm{comb}\left(\frac{x}{p}\right), \tag{1}$$

* Corresponding author.
E-mail address: j.albero@umh.es (J. Albero).

0143-8166/$ - see front matter © 2012 Elsevier Ltd. All rights reserved.
http://dx.doi.org/10.1016/j.optlaseng.2012.09.004

where $\otimes$ denotes the convolution operation; the comb($\cdot$) function is defined as

$$\mathrm{comb}\left(\frac{x}{p}\right) = p\sum_{n=-\infty}^{n=+\infty}\delta(x-np), \tag{2}$$

being p the period of the grating, and

$$g_0(x) = \exp\left(i\frac{2\pi x}{p}M\right)\mathrm{rect}\left(\frac{x}{p}\right), \tag{3}$$

denotes the function defining a single period of the grating (sometimes it is referred to as the slit function [10,11]). The rect(x) function is defined as 1 if $|x|<1$, and zero elsewhere. The blazed grating phase profile is sketched in Fig. 1(a). The parameter M in Eq. (3) controls the phase dynamic range of the blaze grating. The phase ramp has a maximum variation $\Phi_{\max}=2\pi M$; the standard blazed grating ($\Phi_{\max}=2\pi$) is obtained for $M=1$.

The intensity of the Fourier transform of Eq. (1) is given by

$$I(u) = \left|G_0(u)\right|^2\frac{1}{p^2}\mathrm{comb}\,(up), \tag{4}$$

where $G_0(u)$ is the Fourier transform of $g_0(x)$, u denoting the spatial frequency coordinate. Considering the slit function in Eq. (3), its Fourier transform squared modulus can be expressed as:

$$\left|G_0(u)\right|^2 = p^2\mathrm{sinc}^2(p(u-Mu_1)), \tag{5}$$

where $u_1=1/p$ is the fundamental frequency of the grating (first harmonic order). The sinc function is defined as $\mathrm{sinc}(x)=\sin(\pi x)/(\pi x)$. The relative intensity I_n of each diffraction order is given by the function $I(u)$ evaluated at the harmonic frequencies $u_n=nu_1$, $n=0,\pm1,\pm2\ldots$. In this case, for an arbitrary value of M, they are given by:

$$I_n = \mathrm{sinc}^2(n-M) \tag{6}$$

In order to intuitively understand the phenomena, Fig. 1(b) shows a profile of the functions comb(up), $\mathrm{sinc}^2(p(u-Mu_1)$ and $I(u)$, for a value $M=1.5$. Note that the comb function gives the position of the diffracted orders at locations $u_n=nu_1$. The squared sinc function is an envelope function that modulates the relative intensity of the diffraction orders. The position of this envelope function is controlled by the M parameter, being the maximum located at the spatial frequency $u=Mu_1$. For instance, for $M=1$ ($\Phi_{\max}=2\pi$) and for $M=2$ ($\Phi_{\max}=4\pi$), the maximum of this envelope function is centered at the first (u_1) and at the second ($u_2=2u_1$) harmonic orders, respectively. And the zeros of the sinc function exactly coincide with the rest of harmonic frequencies u_n. Thus, the light is fully diffracted either onto the first ($n=1$) or onto the second ($n=2$) diffraction order in each case.

Values of M lower than one lead to a diffraction pattern where the most intense orders are $n=0$ and $n=1$. For instance, for $M=0.5$, $I_0=I_1=40.5\%$. This situation ($M<1$) has been analyzed in SLM devices showing a limited phase modulation range, less than 2π radians [6]. The spatial variation of this M parameter has been a very useful technique to encode amplitude information onto a phase only function [12], however, always limited to the range (0,1). Here, on the contrary, we consider extending the typical (0,1) range to values $1<M<2$, where the envelope function is centered between the first and the second harmonic orders, thus being both of them the most intense ones. For instance, for $M=1.5$, $I_1=I_2=40.5\%$. Next, we present experimental verification of this Fourier theory.

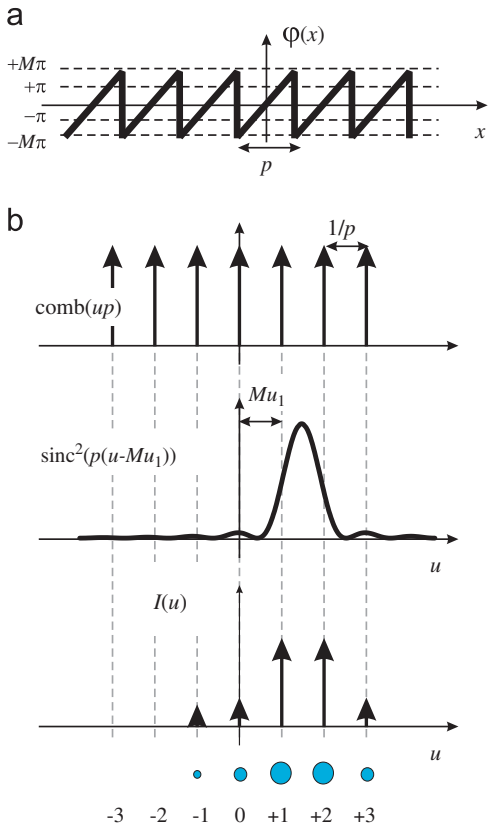

Fig. 1. (a) Phase profile $\varphi(x)$ of the blazed grating. Parameter M controls the phase dynamic range and (b) different functions involved in the generated Fourier pattern.

3. Experimental results with a large phase modulation LCoS display

We have experimentally generated such blazed gratings with a parallel-aligned Hammamatsu LCoS-SLM (X10468 series), with 792×600 pixels of size $20\times20\ \mu m^2$. The rise and fall response times at a wavelength of 633 nm are 10 ms and 35 ms, respectively, which can be assumed similar for the device recommended range of operation (from 400 nm to 700 nm). The polarization of the input beam was selected as linearly polarized along the liquid crystal director axis, in order to obtain a phase-only modulation output. In that configuration, this LCoS-SLM provides a modulation depth range from around 2.3π at 700 nm to 6.4π. We measured the phase modulation range versus the addressed grey level at typical wavelengths using a calibration method based on displaying a two-level grating on the LCoS and measuring the intensity of the zero and first diffraction orders [13]. For the operating wavelengths $\lambda=633$ nm (He–Ne laser), $\lambda=514$ nm and $\lambda=454$ nm of a tunable Ar ion laser, we obtained 2.4π rad, 3.2π rad and 4π rad phase modulation range, respectively. The latter has been used in this work to illuminate the SLM display. From the measured values, fitting models can be used to predict phase changes at other wavelengths in the range [14]. Once the device was calibrated, blazed gratings with different M parameter were displayed on the SLM, by addressing adjusted gray level images via PC. The corresponding diffraction patterns were captured with a CCD camera, (Basler, scA1390-17fc, with 1392×1040 pixels).

Fig. 2 shows the experimental result with a grating with period $p=64$ pixels, where we progressively increase the phase depth to have values $\Phi_{\max}=0$, π, 2π, 3π and 4π, respectively (steps of 0.5 in the M parameter). The experiments are performed in equal conditions and show agreement with Eq. (6). We calculated, in each case, the diffraction efficiency η_k as the intensity of the kth diffracted order respect to the incident light on the SLM.

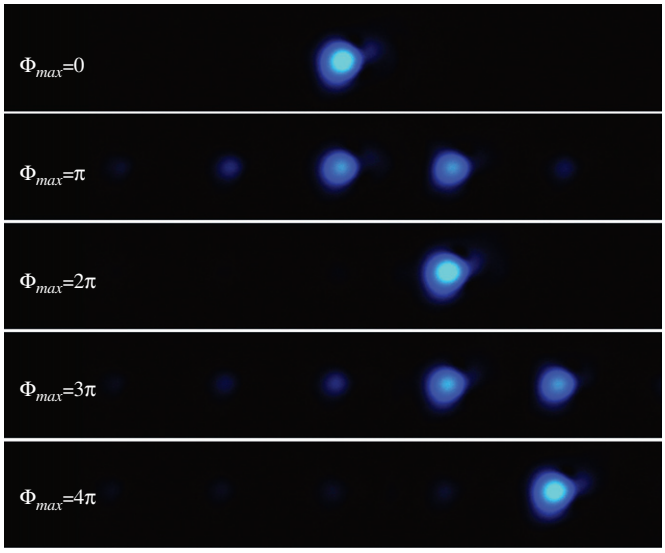

Fig. 2. Diffraction patterns generated by blazed gratings with different phase modulation range Φ_{max}. The period of the gratings is of 64 pixels.

Therefore, loses due to the intrinsic absorption and diffraction by the pixel array structure are taken into account. The trivial case when $\Phi_{max}=0$ indicates the system optical axis through the zero diffraction order with $\eta_0=0.673$. When $\Phi_{max}=\pi$, most of the energy is split between the zero and first diffraction orders ($\eta_0=0.308$ and $\eta_1=0.300$), and some additional energy is spread onto other weak orders. When $\Phi_{max}=2\pi$, the expected deflection onto the first diffraction order is obtained ($\eta_1=0.669$). For $\Phi_{max}=3\pi$, the intensity is now mainly split among the first and second diffraction orders ($\eta_1=0.280$ and $\eta_2=0.275$). Finally, for $\Phi_{max}=4\pi$, all the energy is now concentrated on the second diffraction order ($\eta_2=0.565$). The slight difference between the efficiencies at $\Phi_{max}=0$ and $\Phi_{max}=4\pi$ may be expected because of the possible deviation from the perfect 4π linear phase-only modulation at the operating wavelength.

Note that this last situation is equivalent to a different blazed grating with $\Phi_{max}=2\pi$, but with a period $p'=p/2$. The blazed grating with 4π phase modulation operating in the second harmonic order is equivalent to the blazed grating with 2π phase modulation with half the period. This result is interesting from the practical point of view, since it increases the effective spatial resolution of the devices by a factor of two, which might be a critical issue in applications requiring high resolution. So, large phase modulation depth permits implementing continuous phase DOE elements with less resolution requirements. It is also interesting since some LC-SLMs present electronic effects that cause a reduction of the diffraction efficiency when short period gratings are displayed (the effective phase modulation is reduced) [9]. This is in fact the case of our device. For instance, we measured a reduction of the effective phase modulation to only 3.65π radians for gratings with 8 pixel periods, similar to the results presented in Ref. [8]. Note that the large period of 64 pixels selected in Fig. 2 avoids this effect and the results there reproduce very well the theory presented in the previous section. However, this electrical artifact produces a considerable reduction of the diffraction efficiency when DOEs with short periods are displayed, and a specific phase encoding technique was proposed to compensate this effect in Ref. [8].

Here we take profit from operating in the second harmonic component to reduce this effect, in this case applied to diffractive lenses. Indeed, the so-called multi-order [15] or harmonic [16] diffractive lenses are higher generalizations of the usual modulo 2π blazed diffractive lens, and they were used to design lenses

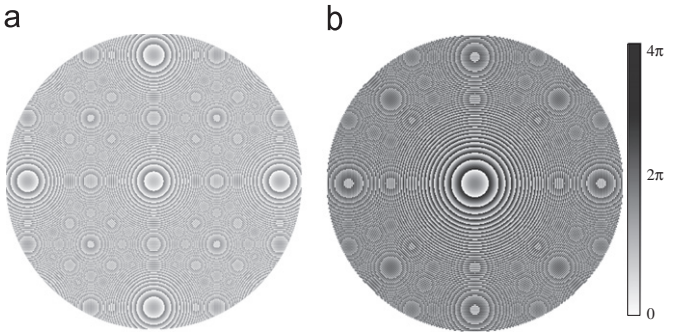

Fig. 3. Encoded diffractive lenses. (a) $f=150$ mm focal length and 2π phase modulation range and (b) $f=300$ mm focal length and 4π phase modulation range.

with specific spectral properties. The ease of fabrication thanks to keeping surface features large compared to wavelength was mentioned in Refs. [15,16] as a goal. Diffractive lenses have been demonstrated onto twisted nematic LCoS displays [17,18]. However, the above mentioned higher order diffractive lenses has not been reproduced with SLMs due to the strong limitations in the available phase modulation dynamic range.

The phase mask of the lens to be encoded onto the SLM is given by

$$L(r)=\exp\left(i\frac{\pi r^2}{\lambda f}\right), \tag{7}$$

where $r=\sqrt{x^2+y^2}$ is the radial coordinate, and f is the lens focal length. The efficient encoding of such diffractive lenses is limited by the spatial resolution of the display. Indeed, a nominal limit has been defined as the Nyquist focal length, f_N, as [19]:

$$f_N=\frac{N\Delta^2}{2\lambda} \tag{8}$$

where Δ denotes the pixel spacing and where an $N\times N$ array of square pixels is assumed to display the pattern. Although shorter focal lengths can be encoded, they result in less efficient patterns. Moreover, lenses with large focal length also decrease the quality, since a reduced number of phase rings can be encoded onto the display. In addition, quantization levels affect the efficiency of the focalization as well. An arbitrary definition range of focal lengths has been proposed as $f_N<f<50f_N$ [19]. In our system, the Nyquist focal length is $f_N=168$ mm.

Fig. 3(a) shows an example of such a diffractive lens, with a focal length $f=150$ mm, slightly below f_N in our system. The resolution limitations are clearly visible in the form of spurious additional lenses that appear in the vertical and horizontal directions. These spurious lenses will focus at additional off-axis points in the same focal plane, thus reducing the efficiency of the main focal spot [19,20]. As we mentioned before, a solution to that spurious focal points might be to increase the focal length of the diffractive lens. In Fig. 3(b) we show a lens that is encoded with $f=300$ mm, i.e., twice the previous focal length (thus larger than f_N). Note that both phase masks present very short periods in the outer part, and therefore diffracted patterns will be very much affected by the efficiency loss caused by the use of high spatial frequencies. However, the resolution requirements of the 300 mm focal length lens are reduced in comparison with the 150 mm focal length lens.

Following the theory in Ref. [6], the second harmonic component of a diffractive lens focuses at a distance $f_2=f/2$. Therefore, if the lens in Fig. 3(b) is displayed with a 4π modulation range, it will provide the main focus at the same plane than the lens in Fig. 3(a) displayed with a 2π modulation range. For the sake of clarity we have explained that situation in Fig. 4. In Fig. 4(a) the lens is encoded

with $f_1=150$ mm and 2π phase modulation. If illuminated with a collimated beam, it will focus at the plane F_1 located 150 mm from the SLM plane. In Fig. 4(b) the lens is encoded with $f_1=300$ mm and 4π phase modulation. The first harmonic would focus at the plane F_1, which is now moved 300 mm from the SLM plane. The second harmonic component focalization (F_2) will be at the same plane, i.e., $f_2=300/2=150$ mm. Therefore, if the lens in Fig. 4(b) is displayed with a 4π phase modulation, it will provide a focalization at the same plane as the lens in Fig. 4(a) displayed in the regular way (2π phase modulation). But a better efficiency is expected in former case.

Experimental verification is presented in Fig. 5. We used the same LCoS display to generate such lenses. In Fig. 5(a) and (b) we show the experimental capture of the focal plane at a distance $z=150$ mm, when these two lenses are addressed onto the SLM. The result, captured in the same exact conditions, shows the expected spurious focalizations. However, note that diffractive lens replicas are more significant for the 2π lens (Fig. 5(a)) than for the 4π lens (Fig. 5(b)). In order to enhance the visualization of this efficiency improvement, we show below each image the corresponding intensity profile along the horizontal line covering these focalizations. A significant reduction of approximately 55% in the intensity of the secondary focalizations is measured, thus providing a much more efficient main focalization. Moreover, oblique spurious focalizations disappear almost completely.

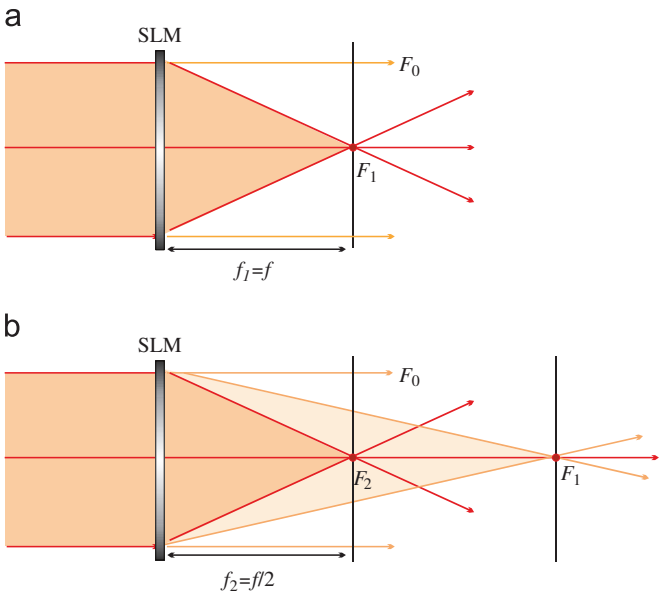

Fig. 4. Optical setups for the visualization of focused beams: (a) with the 2π diffractive lens ($f=150$ mm) and (b) with the 4π diffractive lens ($f=300$ mm).

Note that in Fig. 5(b) there is low but nevertheless noticeable external light contribution around the on-axis focus. This effect can be easily explained with Fig. 4(b). Although we encoded the lens to reach 4π phase modulation, due to the presence of very short periods in the image, there is some amount of energy contributing to the first harmonic component. Therefore, besides the main focalization in the second harmonic focal plane F_2, there is some light focusing in the first order, i.e., plane F_1, which appears defocused in plane F_2, and contributes as a noise surrounding the main focus. This effect will be significantly reduced if the focal distances used for encoding the diffractive lenses are clearly far from the Nyquist focal distance.

4. Conclusions

In summary, we have reproduced second order diffractive optical elements using a pixelated phase-only SLM with a large phase modulation depth, which reaches 49π radians for the wavelength $\lambda=454$ nm. We presented a Fourier transform analysis for blazed diffraction gratings with arbitrary modulation depth, and we provided experimental results that verify the presented theory. We established the equivalence of operating in the second harmonic component (4π phase modulation) with half spatial frequency. The technique has been then applied to diffractive lenses, where we showed an improvement of focusing diffraction efficiency. A significant reduction of spurious replicated lenses is achieved.

Future experiments using broadband illumination for reducing the chromatic aberrations that exhibit diffractive lenses are under consideration. SLMs with even larger phase modulation can be

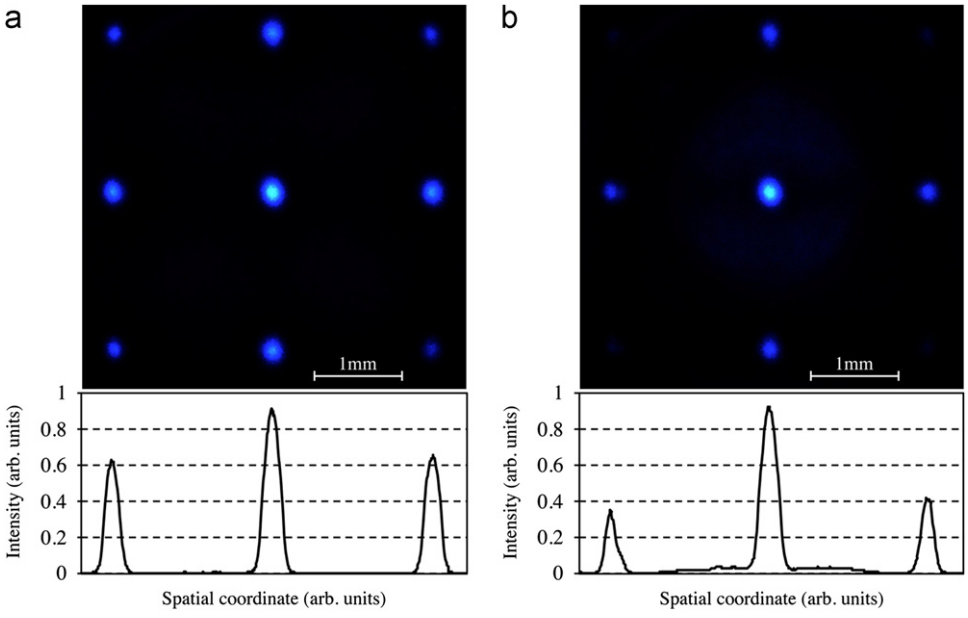

Fig. 5. Experimental result captured at the focal plane ($z=150$ mm) when the lens in (a) is encoded with phase modulation $\Phi_{max}=2\pi$ (Fig. 3(a)), and (b) when the lens in is encoded with phase modulation $\Phi_{max}=4\pi$ (Fig. 3(b)). A 1D profile covering the main focus as well as other secondary axial focal points is included.

useful to reproduce programmable diffractive lenses with schemes similar to those in Refs. [12,13]. Using larger phase modulation depth can also be useful to reduce electrode resolution requirements in systems with liquid crystal microlenses [21].

Acknowledgements

The authors acknowledge financial support from the Spanish Ministerio de Ciencia e Innovación (grant FIS2009-13955-C02-02). JA acknowledges the financial support from the Spanish Ministerio de Educación of Spain through the Programa Nacional de Movilidad de Recursos Humanos del Plan Nacional de I+D+i 2008–2011.

References

[1] Goodman J. Introduction to Fourier optics. 3rd ed.. Greenwood Village: Roberts and Company Publishers; 2004.
[2] Yeh P, Gu C. Optics of liquid crystals displays. 2nd ed.. West Sussex: John Wiley & Sons; 2010.
[3] Konforti N, Marom E, Wu S-T. Phase-only modulation with twisted nematic liquid-crystal spatial light modulators. Opt Lett 1988;13:251–3.
[4] Efron U, Wu S-T, Bates TD. Nematic liquid crystals for spatial light modulators: recent studies. J Opt Soc Am B 1986;3:247–52.
[5] Davis JA, Moreno I, Tsai P. Polarization eigenstates for twisted-nematic liquid crystal displays. Appl Opt 1998;37:937–45.
[6] Moreno I, Iemmi C, Márquez A, Campos J, Yzuel MJ. Modulation light efficiency of diffractive lenses displayed on a restricted phase-mostly modulation display. Appl Opt 2004;43:6278–84.
[7] Martínez JL, Moreno I, Davis JA, Hernández TJ, McAuley KP. Extended phase modulation depth in twisted nematic liquid crystal displays. Appl Opt 2010;49:5929–37.
[8] Márquez A, Iemmi C, Moreno I, Campos J, Yzuel MJ. Anamorphic and spatial frequency dependent phase modulation on liquid crystal displays. Optimization of the modulation diffraction efficiency. Opt Express 2005;13:2111–9.
[9] Márquez A, Moreno I, Iemmi C, Campos J, Yzuel MJ. Electrical origin and compensation for two sources of degradation of the spatial frequency response exhibited by liquid crystal displays. Opt Eng 2007;46:114001.
[10] Born M, Wolf E. Principles of optics. 7th ed. Cambridge: Cambridge University Press; 1999 Section 8.6.1. diffraction gratings.
[11] Martínez A, Sánchez-López MM, Moreno I. Phasor analysis of binary amplitude gratings with different fill factor. Eur J Phys 2007;28:805–16.
[12] Davis JA, Cottrell DM, Campos J, Yzuel MJ, Moreno I. Encoding amplitude information onto phase-only filters. Appl Opt 1999;38:5004–13.
[13] Zhang Z, Lu G, Yu FTS. Simple method for measuring phase modulation in liquid crystal television. Opt Eng 1994;33:3018–22.
[14] Wu S-T. Birefringence dispersions of liquid crystals. Phys Rev A 1986;33:1270–2174.
[15] Faklis D, Morris GM. Spectral properties of multiorder diffractive lenses. Appl Opt 1995;34:2462–8.
[16] Sweeney DW, Sommargren GE. Harmonic diffractive lenses. Appl Opt 1995;34:2469–75.
[17] Wang X, Dai H, Xu K. Tunable reflective lens array based on liquid crystal on silicon. Opt Express 2005;13:352–7.
[18] McManamon PF, Dorschner TA, Corkum DL, Friedman LJ, Hobbs DS, Holz M, et al. Optical phased array technology. Proc IEEE 1996;84:268–98.
[19] Cottrell DM, Davis JA, Hedman TR, Lilly RA. Multiple imaging phase-encoded optical elements written as programmable spatial light modulators. Appl Opt 1990;29:2505–9.
[20] Carcolé E, Campos J, Bosch S. Diffraction theory of Fresnel lenses encoded in low-resolution devices. Appl Opt 1994;33:162–74.
[21] Algorri JF, Urruchi V, Sánchez-Pena JM, Bennis N, Geday MA. Liquid crystal microlenses with gradient refraction index control. Opt Pura Apl 2012;45:71–8.